Proceedings of Dynamic Systems and Applications 6 (2012) 241–247

Robustness of Action Potentials in Cardiac Myocytes

Chuan Li[1], Vasilios Alexiades[2] and Jack W. Buchanan[3]

[1]Mathematics, University of Tennessee, Knoxville TN, USA
[2]Mathematics, University of Tennessee, Knoxville TN, USA and Oak Ridge National Laboratory, Oak Ridge TN, USA
[3]Biomedical Engineering and Medicine, University of Tennessee Health Science Center, Memphis TN, USA

ABSTRACT: Action potentials are voltage waveforms propagating along excitable tissues, such as neurons and cardiac myocytes. They are described by the "cable" equation, a parabolic diffusion-reaction PDE for the transmembrane potential, coupled to a system of ODEs for the ionic currents across the cell membrane, constituting the reaction term of the PDE.

We present simulations of action potentials, with Luo-Rudy ionic model, for normal and abnormal tissue, exploring effects of various parameters, towards modeling ischemia and arrhythmia.

AMS (MOS) Subject Classification. 35K57, 65N08, 65N40, 92C30

1 INTRODUCTION

Electrical propagation (action potentials) in human cardiac tissue can be described mathematically by a nonlinear parabolic diffusion-reaction equation for the transmembrane potential (voltage) $V(x,t)$, known as the *cable equation* ([3, 8])

$$C_m \frac{\partial V}{\partial t} = \frac{1}{R_a}\frac{\partial^2 V}{\partial x^2} - I_{ion}(V,t) - I_{stim}(t), \tag{1}$$

where R_a and C_m are the axial resistance and membrane capacitance, I_{ion} represents the total ionic current, and $I_{stim}(t)$ is an applied stimulus current which instigates an action potential.

The source term I_{ion} is usually specified by some Hodgkin-Huxley type ionic model. In our simulations, we use the *Luo-Rudy phase I (1991) model*, one of the most widely used models for cardiac myocytes. It consists of six ionic currents generated by sodium (Na^+), potassium (K^+), and calcium (Ca^{2+}) ions, [7], (while the original Hudgkin-Huxley model has only three, [2]):

$$I_{ion}(V) = I_{Na}(V) + I_{SI}(V) + I_K(V) + I_{K1}(V) + I_{Kp}(V) + I_b(V), \tag{2}$$

where I_{Na} is a *fast sodium current*, inducing fast upstroke and slow recovery after inactivation; I_{SI} is a *slow inward current*; I_K is a *potassium current*; I_{K1} is a *potassium current* that includes a negative-slope phase; I_{Kp} is a *plateau potassium current*; and I_b is a *time-independent background current*.

These currents depend on seven activation and inactivation "gates", traditional denoted as m ,h , j, d, f, X, Cai, each of which is governed by an ODE of the form

$$\frac{dg}{dt} = \alpha_g(V)(1-g) - \beta_g(V)g, \quad g = m,\ h,\ j,\ d,\ f,\ X,\ Cai. \tag{3}$$

The α's and β's, taking values between 0 and 1, are specified by (messy) explicit formulas as functions of voltage V. We used the curated version *luo_rudy_1991_version06* from [1].

Membrane capacitance is fixed in all simulations at $C_m = 1.2\ \mu F/cm^2$. Cytoplasmic resistance $R_a = 300\ k\Omega$ results from resistivity $R_i = 150\,\Omega\,cm$ inside human cardiac cells, [3]. Biological experiments have indicated that "gap junctions" connecting adjacent cells present much greater resistance to current flow between cells, [9]; thus gap junction resistivity R_{gap} would be much higher, but no precise values are available. Therefore, in our simulations, the "normal" value $R_i = 150\,\Omega cm$ is held fixed and R_{gap} is varied to unveal its effects. As boundary conditions, we assume zero voltage gradient at the ends of the cable, and initialize the system from steady state as described in the Appendix.

The mathematical model is then completely described by the PDE (1), the seven ODEs (3), and the above initial setup and boundary conditions.

By finite volume discretization in space, the PDE is reduced to an ODE at each control volume. With M control volumes, a system of $8 \times M$ highly nonlinear ODEs needs to be solved using some numerical time-integrator. We have implemented and tested eleven time-stepping schemes (low and high order, explicit and implicit, non-adaptive and adaptive). Results and comparisons of serial implementations were reported in papers [4, 5].

Cardiac cells (each of length $30 - 130\,\mu m$) are arranged in bundles (of thousands of cells), referred to as "cables". To capture the rapid change of voltage (and gates), fine mesh is necessary (of the order of $10\ \mu m$) and evaluation of I_{ion} is very costly. Thus, simulations on cables of realistic lengths ($50\ mm$ or greater) are very slow, calling for parallel computing.

Parallelization via spatial domain decomposition and the MPI library for distributed memory multiprocessors (clusters) has been implemented and some results of our parallel experiments were reported in [6]. The efficiency resulting from parallelization enables us to carry out extensive biological simulations and parametric studies on cables of various lengths.

The simulations reported below were performed on 250 CPUs of the Frost cluster of NICS at ORNL (which has 2048 Intel Xeon 2.8 GHz processors in 128 16-core nodes), using fine mesh of $\Delta x = 8\,\mu m$ on cables of length $50\,mm$ (grid of 6250 control volumes).

Certain quantities pertaining to an action potential are characteristic of the cell and the ionic currents, and independent of the stimulus, cable length, and locations used for measurement. Thus these quantities also serve as accuracy indicators on the numerical schemes. Such important quantites, which are tracked in our simulations, are the following:

- **Action Potential Duration (APD):** The duration is determined by measuring how long the potential V at a specific location stays above a certain cut-off value. In our computations, APD is determined by setting a cut-off voltage at 90% of the initial equilibrium voltage.
- **Propagation Velocity:** It measures how fast the action potential propagates along the cable. It is measured by the difference of the starting time of APs at two specified locations.
- **Maximum voltage** (V_{max}) and **maximum rate of change** (dV/dt_{max})**.**

To visualize the propagation of action potentials, we output V at five equispaced points along the cable (at $x = 0, L/4, L/2, 3L/4, L$, with L = cable length).

2 SIMULATIONS WITH NORMAL PARAMETER VALUES

First we present the base case of normal parameters, with $[K]_o = 5.4\,mM$ and $Ri = R_{gap} = 150\,\Omega\,cm$. Single or repeated stimulus (of various periods) was applied in a small ($10\,\mu m$) region at the left end of the cable.

In a first set of tests, we applied single stimulus of various strengths on the same cable. No action potential is elicited unless the stimulus is above a certain threshold. This is the "all-or-nothing" property [10] of action potentials.

When the stimulus is strong enough to depolarize the stimulated site (to positive potential), an action potential is generated which then propagates down the length of the cable. Figure 1a shows voltage history at five equally spaced nodes. Note that the curves are not singular, as seen in the zoom-in plot of the upstroke at the right-end of the cable in Figure 1b. Voltage profiles at several times are shown in Figure 2a and corresponding gates history in Figure 2b. A

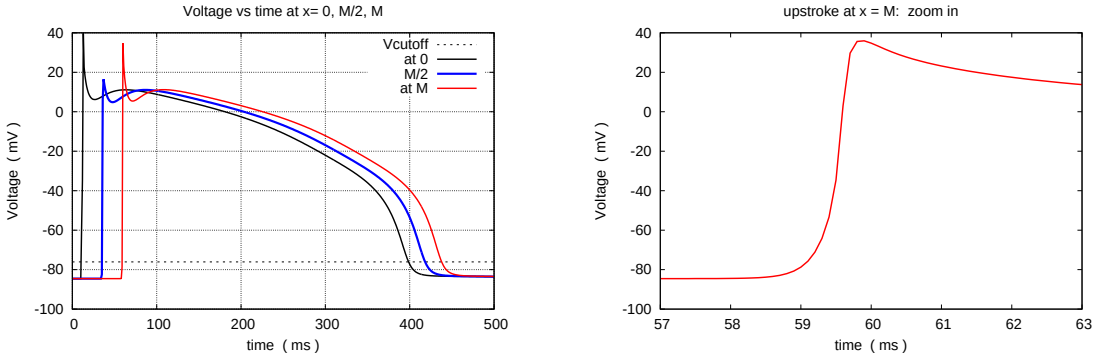

(a) Voltage vs time at 5 equally spaced nodes

(b) Zoom-in at upstroke of AP at right-end of cable

Figure 1: Action potential on a cable of length $50\,mm$

crucial property of excitable cells is "refractoriness", which prevents the generation of new action potential while the cell is still depolarized. The next series of tests were designed to exhibit this property by altering the stimulus period. Some results are shown in Figure 3. The action potential duration shown in Figures 3a - 3b is about $400\,ms$. In Figure 3a, one can see that the 2nd stimulus (at $350\,ms$), occurring inside the refractoriness period of the 1st stimulus, did not propagate. Instead, the next action potential is evoked by the 3rd stimulus (at $700\,ms$). The same phenomenon can be observed with the 4th stimulus in Figure 3b where stimulus period is $200\,ms$. Figure 3 demonstrates refractoriness of the action potential, as well as the remarkable robustness of its shape.

3 SIMULATIONS WITH ABNORMAL PARAMETER VALUES

In our parametric studies we varied the following parameters:

- Gap junction resistivity, R_{gap}, which is applied at boundaries between cardiac cells. The normal cytoplasmic resistivity for human myocytes is $Ri = 150\ \Omega cm$ and R_{gap} is considerably higher, but no precise values are known. We tested several higher values: $R_{gap} = 300, 600, 1000, 2000\ \ \Omega cm$.
- External concentration of potassium $[K]_o$. The normal value is $[K]_o = 5.4\ mM$. We tested both lower values (=3, 4) simulating conditions of **hypokalemia**, and higher values (=7, 8, 9, 10, 11, 12, 13) simulating conditions of **hyperkalemia**.

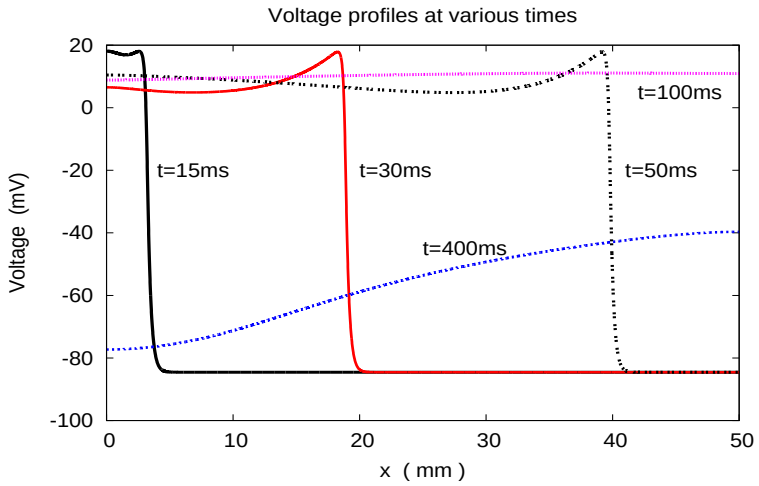

(a) Voltage profiles at 15, 30, 50, 400 ms

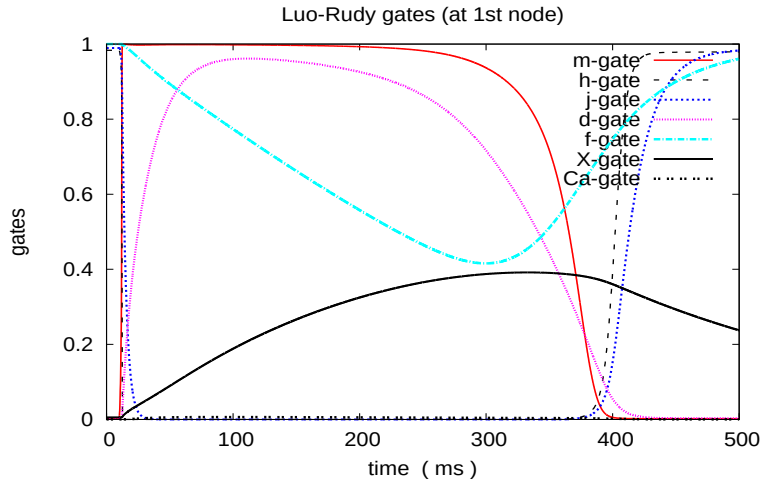

(b) Gates vs time at first node.

Figure 2: Voltage profiles and gates history on a cable of length $50\ mm$

Their influence on the biological quantities, namely, action potential duration (APD), propagation speed ($speed$) and maximal potential (V_{max}) were monitored and will be presented below.

First, we study the effect of R_{gap} on the main biological quantites, keeping $[K]_o = 150\, mM$. Results at the middle of the cable appear in Figures 4a - 4d. From these figures, we can see that (a) R_{gap} does not change the shape of the actions potential, but higher R_{gap} delays the upstroke, as expected. (b) The action potential duration is very robust and R_{gap} has little effect on it. APD remains almost constant as R_{gap} is varied. (c) Higher R_{gap} decreases the propagation speed. (d) R_{gap} increases V_{max} significantly.

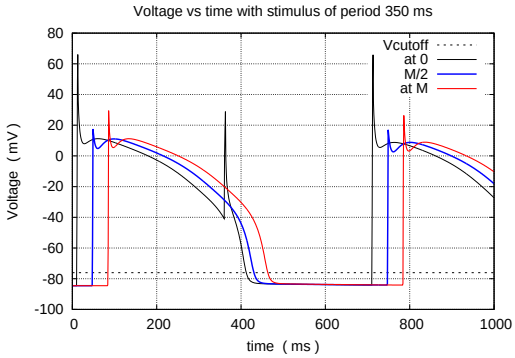

(a) Frequent stimulations of period $350\ ms$

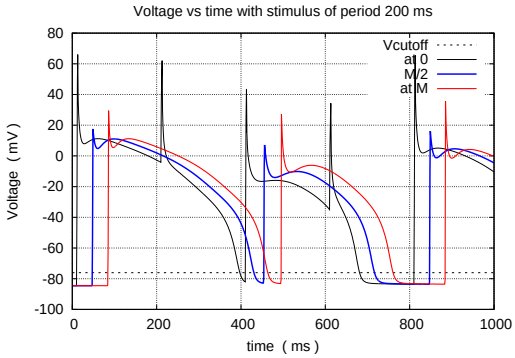

(b) Frequent stimulations of period $200\ ms$

Figure 3: Simulation of refractoriness on a cable of length $50\ mm$

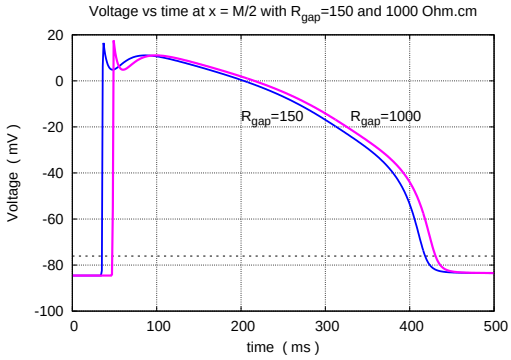

(a) Effect of R_{gap} on potential

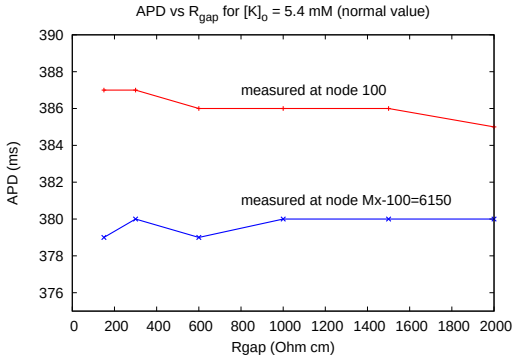

(b) Effect of R_{gap} on APD

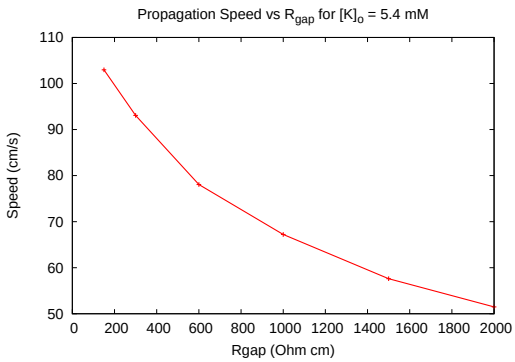

(c) Effect of R_{gap} on propagation speed

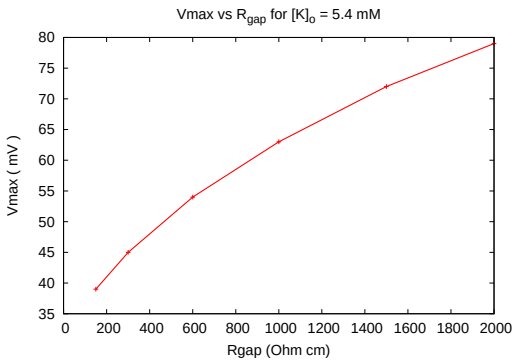

(d) Effect of R_{gap} on V_{max}

Figure 4: Effect of R_{gap} on biological quantities

The above simulations were with normal $[K]_o = 5.4\,mM$. To detect the effect of abnormal $[K]_o$ and of R_{gap}, we repeated the above simulations with various $[K]_o$ and R_{gap} values. Selected representative results are shown in Figures 5a - 5d. They show that R_{gap} has similar effect as in the normal $[K]_o$ case, and that abnormal $[K]_o$ affects APD, propagation speed and V_{max} significantly.

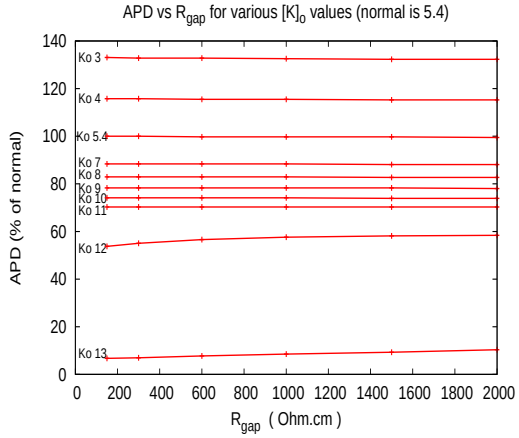

(a) Effect on APD

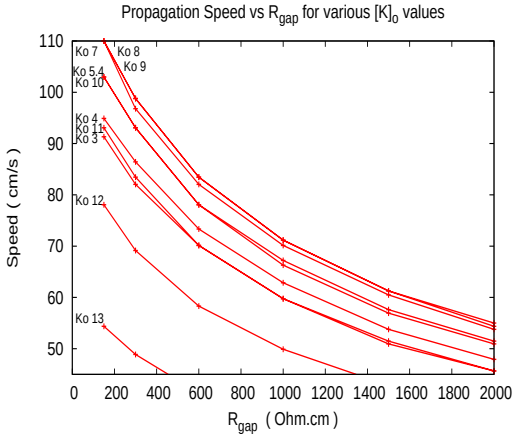

(b) Effect on propagation speed

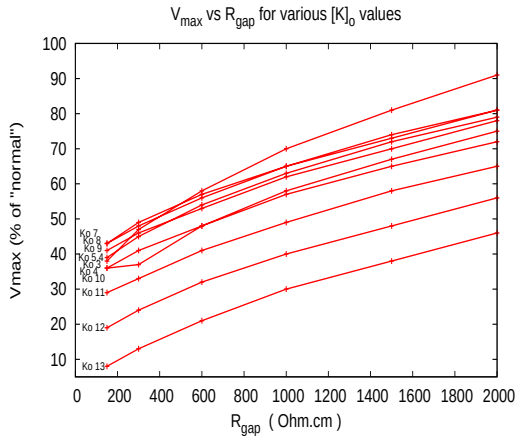

(c) Effect on V_{max}

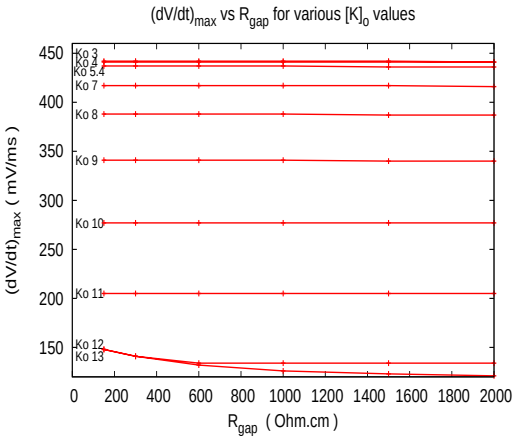

(d) Effect on dV/dt_{max}

Figure 5: Effect of varying R_{gap} and $[K]_o$.

Finally, we explore what happens if only a portion of the cable is exposed to abnormal $[K]_o$. For each of the abnormal $[K]_o$ values: 3, 4, 7, 8, 9, 10, 11, 12, 13 mM, we performed seven simulations, with the abnormal value applied to a different portion of the cable and in different parts, e.g. in the left third, the right third, left two thirds, middle two thirds, right two thirds, etc. This set of 63 simulations attempts to capture the variability of APD, propagation speed and V_{max}, which are visualized by the red vertical segments in Figures 6a - 6c. We see that the greater the $[K]_o$, the greater the variability, which becomes extreme at $[K]_o = 11$.

4 CONCLUSIONS AND FUTURE WORK

These experiments on one-dimensional cables suggest that abnormal $[K]_o$ values, placed in a portion of two- or three-dimensional tissues, may have significant effect on action potential propagation and drive it into irregular patterns. In fact, two-dimensional simulations have been performed and verified this guess. These results will be reported elsewhere.

5 ACKNOWLEDGMENTS

This work was supported by NIH grant 1R21GM080698-01A1. This research used resources of the Oak Ridge Leadership Computing Facility at the National Center for Computational Sciences (NICS) at Oak Ridge National Laboratory, which is supported by the Office of Science of the Department of Energy under Contract DE-AC05-00OR22725.

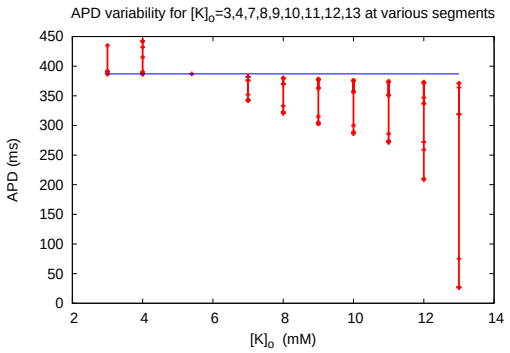

(a) Variability of APD.

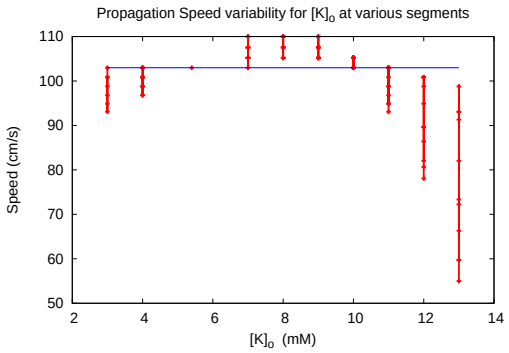

(b) Variability of propagation speed.

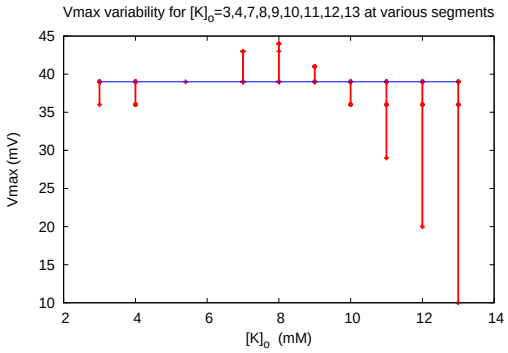

(c) Variability of V_{max}.

Figure 6: Effect of $[K]_o$ on biological quantities.

REFERENCES

[1] cellML, model *luo_rudy_1991* , (accessed on 2 Sep.2011), CellML author: Catherine Lloyd http://models.cellml.org/exposure/2d2ce7737b42a4f72d6bf8b67f6eb5a2/luo_rudy_1991.cellml/view

[2] AL Hodgkin and AF Huxley, A quantitative description of membrane current and its application to conduction and excitation in nerve, *J. Physiol.*, 117: 500–544, 1952.

[3] James Keener and James Sneyd, *Mathematical Physiology*, Springer, 1998.

[4] C Li and V Alexiades, Comparison of time stepping schemes on the cable equation. *Electron. J. Diff. Eqns., Conference*, 19: 189-196, 2010.

[5] C Li and V Alexiades, Time stepping for the cable equation, Part 1: Serial performance. *Proceedings of Neural, Parallel & Scientific Computations*, 4: 241-246, 2010.

[6] C Li and V Alexiades, Time stepping for the cable equation, Part 2: Parallel performance. *Proceedings of Neural, Parallel & Scientific Computations*, 4: 247-251, 2010.

[7] CH Luo and Y Rudy, A model of the ventricular cardiac action potential: depolarization, repolarization, and their interaction. *Circulation Research*, 68: 1501–1526, 1991.

[8] R Plonsey and RC Barr, *Bioelectricity, a quantitative approach*, 3rd ed., Springer, 2007.

[9] RM Shaw and Y Rudy, Electrophysiologic effects of acute myocardial ischemia: a theoretical study of altered cell excitability and action potential duration. *Cardiovascular Res.*, 35(2): 256–272, 1997.

[10] Wikipedia, http://en.wikipedia.org/wiki/Action_potential

APPENDIX

The external potassium concentration $[K]_o$ enters several of the ionic currents in (2). Each value of $[K]_o$, assumed to hold everywhere, determines a resting (steady) state, which we compute by a simulation starting from arbitrary initial values *without applying any stimulus*. The computed rest values for the potential V and the gates, associated with normal and several abnormal $[K]_o$ values, are listed in TABLE 1. They are used as initial values for simulations.

Table 1: Initial values for simulations

$[K]_o$	**5.4 (normal)**	**3.0 (abnormal)**	**4.0 (abnormal)**	**7.0 (abnormal)**
V	-84.54799678282664	-96.00223575957419	-90.81551303451198	-78.67973684400134
m	0.00166648217313	0.00024070076809	0.00058200973949	0.00438066429310
h	0.98330219789904	0.99872727894491	0.99590013700613	0.93986515149662
j	0.98952187383367	0.99889732941648	0.99703695298703	0.95809689756957
d	0.00297744387078	0.00114649813087	0.00176092718051	0.00490745454890
f	0.99998123976333	0.99999782305501	0.99999422716513	0.99994345209289
X	0.00564346895260	0.00180173175262	0.00303206018008	0.00998842432493
Cai	0.00017836352928	0.00013243547761	0.00014830982920	0.00022359447247
$[K]_o$	**8.0 (abnormal)**	**9.0 (abnormal)**	**10.0 (abnormal)**	**11.0 (abnormal)**
V	-75.54165652692299	-72.70773238255576	-70.12397264679385	-67.74748787738635
m	0.00728002211552	0.01144339635209	0.01717608198246	0.02479289747129
h	0.88490560164669	0.80201421451890	0.69306674613317	0.56882167821468
j	0.90723546645185	0.82153559019045	0.70569924515929	0.57458900871432
d	0.00643453367652	0.00823835750666	0.01034236960485	0.01277070476184
f	0.99989797475749	0.99982613252835	0.99971727689208	0.99955792433128
X	0.01348050680379	0.01760223313960	0.02236497194614	0.02777227685655
Cai	0.00025791194364	0.00029720770210	0.00034169540110	0.00039158233702
$[K]_o$	**12.0 (abnormal)**	**13.0 (abnormal)**		
V	-65.54718840722101	-63.50059136465195		
m	0.03460798138824	0.04690119914541		
h	0.44498255576699	0.33513708858460		
j	0.44585024710676	0.33317233223800		
d	0.01554927719980	0.01870109003990		
f	0.99933118604069	0.99901664361355		
X	0.03382343582322	0.04050452208904		
Cai	0.00044709573228	0.00050838365402		